EUROPEAN JOURNAL OF COMPUTATIONAL MECHANICS, 2016
VOL. 25, NOS. 1–2, 147–164
http://dx.doi.org/10.1080/17797179.2016.1181041

Taylor & Francis
Taylor & Francis Group

Boundary element analysis of 2D and 3D thermoelastic problems containing curved line heat sources

M. Mohammadi[a], M. R. Hematiyan[b] and A. Khosravifard[b]

[a]Department of Mechanical Engineering, College of Engineering, Shiraz Branch, Islamic Azad University, Shiraz, Iran; [b]Department of Mechanical Engineering, Shiraz University, Shiraz, Iran

ABSTRACT
Temperature and stress analysis of a medium with concentrated heat sources has some important applications in engineering. In this paper, a boundary element method for analysis of two- and three-dimensional thermoelastic problems containing curved line heat sources in isotropic media is presented. In these problems, the heat generation within the problem domain is concentrated over a curved path. In the conventional integral equations of thermoelasticity, the domain integrals are expressed in terms of the temperature function. In this work, modified integral equations, in which the domain integrals are expressed in terms of the heat source function is used. The shape of the curved line heat source and the intensity function along the source can be arbitrary. Temperature, displacement and stress analyses are performed without considering internal points and without any need to find the temperature distribution in the domain. Three numerical examples are presented to show the effectiveness and accuracy of the proposed method for two- and three-dimensional problems. Highly accurate results are obtained by the proposed method. It is concluded that the presented boundary element formulation is more efficient in comparison with the domain methods in which one needs to consider condensed nodes near the curved line heat source.

ARTICLE HISTORY
Received 14 October 2015
Accepted 31 March 2016

KEYWORDS
Boundary element method; thermoelasticity; heat conduction; curved line heat source; non-uniform intensity

1. Introduction

The thermoelastic analysis of problems with point and/or line heat sources has some important applications in electrical heating, modelling of electronic parts, laser heating (Khan & Yilbas, 2004) and internal cooling of single crystal alloys (Shiah, Guao, & Tan, 2005). Numerical methods are usually used for analysis of practical thermoelastic problems. The boundary element method (BEM) is an attractive and accurate tool for analysis of thermoelastic problems. The research on the boundary element analysis of thermoelastic problems started from 1977

CONTACT M. R. Hematiyan mhemat@shirazu.ac.ir

(Rizzo & Shippy, 1977) and this subject is still an active area of research; see for example (Chekurin & Sinkevych, 2015; Liu, Li, & Huang, 2014; Ochiai, Sladek, & Sladek, 2013; Shiah & Tan, 2012).

There are limited studies on the modelling and analysis of thermoelastic problems involving heat sources. On the other hand, studies focusing on the thermoelastic problems involving line heat sources are rare. Shiah and Tan (2003) presented a 2D BEM formulation for steady-state anisotropic thermoelastic problems involving uniform heat sources. They transformed the domain integrals exactly into boundary integrals.

Shiah and Lin (2003) and Shiah and Huang (2005) analysed 2D anisotropic thermoelastic problems involving non-uniform heat sources using the multiple reciprocity BEM. Ochiai (2005) presented a triple-reciprocity BEM formulation for 3D thermoelasticity involving non-uniform heat sources. Hematiyan, Mohammadi, Marin, and Khosravifard (2011) presented a BEM for analysis of two- and three-dimensional uncoupled thermoelastic problems involving time- and space-dependent distributed heat sources.

In the conventional boundary element (BE) formulation of thermoelastic problems, the domain integrals are expressed in terms of the temperature rise function. It is usually assumed that the temperature rise function is known over the domain and an attempt is made to evaluate the domain integrals with or without domain discretisation; see e.g. (Cheng, Chen, Golberg, & Rashed, 2001; Gao, 2003). These domain integrals can be exactly transformed to the boundary in the cases where the temperature function is harmonic (Aliabadi, 2002). In problems with a source of heat generation in the domain, the variation of temperature in the domain cannot be expressed by a harmonic function and it can be very complicated. In general cases with an arbitrary temperature function, the domain integrals should be evaluated with special methods such as the dual reciprocity method (Partridge & Brebbia, 1990; Partridge, Brebbia, & Wrobel, 1992), multiple reciprocity method (Neves & Brebbia, 1991; Nowak & Brebbia, 1989), triple reciprocity method (Ochiai, 2001a,b), radial integration method (Gao, 2002; Gao & Peng, 2011), or Cartesian transformation method (Hematiyan, 2007, 2008).

The temperature distribution in domains containing a point or a line heat source may be very complicated. Mohammadi, Hematiyan, and Aliabadi (2010) have formulated the displacement and stress integral equations of thermoelasticity in a form in which domain integrals are expressed in terms of heat source function instead of temperature. By this formulation, the thermoelastic problems can be analysed with no need to find the temperature distribution in the domain.

As previously mentioned, there are only a few published papers regarding thermoelastic problems with concentrated heat sources (point and line heat sources). Shiah et al. (2005) presented a BEM formulation for the thermoelastic analysis of an anisotropic medium with point heat sources. They successfully analysed the problem with a boundary-only discretisation. Hematiyan, Mohammadi, and

Aliabadi (2011) presented a boundary element method for analysis of 2D and 3D thermoelastic problems involving concentrated heat sources. They successfully formulated the problem with boundary-only discretisation; however, they limited their attention to straight-line heat sources with a linear variation of the heat source intensity.

This study presents a boundary element method for analysis of 2D and 3D uncoupled linear thermoelastic problems in isotropic media containing curved line heat sources. The shape of the curved line heat source and its strength along the source can be arbitrary. The presented boundary element formulation for thermoelastic problems with curved line heat sources is more efficient in comparison with domain methods such as meshless methods or the finite element method. An accurate modelling of a curved line heat source using the domain methods requires the use of very condensed nodes near the heat source; however, in this study, only boundary discretisation is required and domain integrals are evaluated without internal cells and without any need to find the temperature distribution through the domain.

2. Integral equations of 2D and 3D steady-state thermoelasticity involving heat sources

The governing equations of steady-state thermoelasticity can be expressed as follows:

$$kT_{,ii}(\mathbf{x}) + g(\mathbf{x}) = 0 \tag{1}$$

$$\sigma_{ij,j}(\mathbf{x}) + b_i(\mathbf{x}) = 0 \tag{2}$$

where T is the temperature rise, k is the thermal conductivity, g is the heat source function, σ_{ij} are components of the stress tensor, b_i are components of body force vector and $\mathbf{x}$ is a point of the domain.

Strain components ε_{ij} in terms of the displacement vector components u_i can be expressed as follows:

$$\varepsilon_{ij} = \frac{1}{2}(u_{i,j} + u_{j,i}) \tag{3}$$

Strain components in terms of stress components can be expressed as follows:

$$\varepsilon_{ij} = \frac{1}{E}\left[(1+\nu)\sigma_{ij} - \nu\delta_{ij}\sigma_{kk}\right] + \alpha T\delta_{ij} \tag{4}$$

where E is Young's modulus, ν is Poisson's ratio and α is the coefficient of linear thermal expansion.

The temperature integral equation of steady-state heat conduction in an isotropic domain Ω with a boundary Γ is expressed as follows (Wrobel, 2002):

$$C(\boldsymbol{\xi})T(\boldsymbol{\xi}) = \int_{\Gamma} \left(T^*(\boldsymbol{\xi}, \mathbf{x}) \frac{\partial T(\mathbf{x})}{\partial n} - T(\mathbf{x}) \frac{\partial T^*(\boldsymbol{\xi}, \mathbf{x})}{\partial n} \right) d\Gamma + \frac{1}{k} \int_{\Omega} T^*(\boldsymbol{\xi}, \mathbf{x}) g(\mathbf{x}) d\Omega \quad (5)$$

where $\boldsymbol{\xi}$ is the source point (singular point) and n represents the direction perpendicular to the boundary. C is a coefficient related to the local geometry at the source point. For an internal source point, $C(\boldsymbol{\xi})$ is 1.0, for a source point located on a smooth boundary, $C(\boldsymbol{\xi})$ is 1/2 and for a boundary source point located at a corner of a 2D problem, $C(\boldsymbol{\xi})$ is $\gamma / 2\pi$ where γ is the corner angle. In this work, 3D problems are analysed using constant quadrilateral boundary elements and each boundary source point is located on a smooth part of the boundary (the middle point of the boundary element) and therefore, $C(\boldsymbol{\xi})$ is 1/2. T^* is the fundamental solution of the Laplace problem, which can be expressed by the following equation in 2D problems (Wrobel, 2002):

$$T^* = \frac{1}{2\pi} \ln \left(\frac{1}{r} \right) \quad (6)$$

and in three dimensions is written as:

$$T^* = \frac{1}{4\pi r} \quad (7)$$

where r is the Euclidian distance between $\boldsymbol{\xi}$ and $\mathbf{x}$.

The displacement integral equation of thermoelasticity without body force can be expressed as follows (Aliabadi, 2002):

$$\begin{aligned} C_{ij}(\boldsymbol{\xi})u_j(\boldsymbol{\xi}) = \int_{\Gamma} \left(U^*_{ij}(\boldsymbol{\xi}, \mathbf{x}) t_j(\mathbf{x}) - S^*_{ij}(\boldsymbol{\xi}, \mathbf{x}) u_j(\mathbf{x}) \right) d\Gamma \\ + \frac{E\alpha}{1-2\nu} \int_{\Omega} T(\mathbf{x}) U^*_{ik,k}(\boldsymbol{\xi}, \mathbf{x}) d\Omega \end{aligned} \quad (8)$$

where, t_j represents the components of the traction vector and C_{ij} are the free-term coefficients. For an internal source point, $C_{ij}(\boldsymbol{\xi})$ is δ_{ij}, for a source point located on a smooth boundary, $C_{ij}(\boldsymbol{\xi})$ is $\delta_{ij} / 2$ and the free-term coefficients for a boundary source point located at a corner point can be evaluated by consideration of rigid body motion (Aliabadi, 2002). For 3D problems with constant quadrilateral boundary elements, the source point is located at the middle point of the boundary element and therefore, $C_{ij}(\boldsymbol{\xi})$ is $\delta_{ij} / 2$. U^*_{ij} and S^*_{ij} in Equation (8) are Kelvin fundamental solutions for displacement and traction, respectively, which can be expressed as:

$$U^*_{ij} = \frac{1}{8\pi G(1-\nu)} \left[(3-4\nu)\delta_{ij} \ln \frac{1}{r} + r_{,i} r_{,j} \right] \quad (9)$$

$$S_{ij}^{*} = \frac{-1}{4\pi(1-\nu)r}\left\{\frac{\partial r}{\partial n}\left[(1-2\nu)\delta_{ij} + 2r_{,i}r_{,j}\right] - (1-2\nu)(r_{,i}n_j - r_{,j}n_i)\right\} \quad (10)$$

for plane strain problems and as:

$$U_{ij}^{*} = \frac{1}{16\pi G(1-\nu)r}\left[(3-4\nu)\delta_{ij} + r_{,i}r_{,j}\right] \quad (11)$$

$$S_{ij}^{*} = \frac{-1}{8\pi(1-\nu)r^2}\left\{\frac{\partial r}{\partial n}\left[(1-2\nu)\delta_{ij} + 3r_{,i}r_{,j}\right] - (1-2\nu)(r_{,i}n_j - r_{,j}n_i)\right\} \quad (12)$$

for 3D problems. G in the above equations represents the shear modulus. It is worth mentioning that a plane stress problem can be analysed as a plane strain problem, by a replacement of material constants (Noda, Hetnarski, & Tanigawa, 2003).

The domain integral in Equation (8) is expressed in terms of the temperature function, i.e. $T(\mathbf{x})$. In the thermoelastic problems with line heat sources, the distribution of the temperature in the domain is very complicated and accurate computation of this domain integral is very difficult. Mohammadi et al. (2010) have converted the domain integral in Equation (8) into a domain integral in terms of the heat source function. They showed that the displacement integral equation in Equation (8) could be expressed as follows:

$$\begin{aligned} C_{ij}(\boldsymbol{\xi})u_j(\boldsymbol{\xi}) = \int_\Gamma \left(U_{ij}^{*}(\boldsymbol{\xi},\mathbf{x})t_j(\mathbf{x}) - S_{ij}^{*}(\boldsymbol{\xi},\mathbf{x})u_j(\mathbf{x})\right)d\Gamma \\ + \tfrac{\alpha(1+\nu)}{8\pi(1-\nu)}\int_\Gamma \left(T\tfrac{\partial\omega_i}{\partial n} - \omega_i\tfrac{\partial T}{\partial n}\right)d\Gamma - \tfrac{\alpha(1+\nu)}{8\pi(1-\nu)k}\int_\Omega \omega_i g(\mathbf{x})d\Omega \end{aligned} \quad (13)$$

For plane strain problems ω_i is:

$$\omega_i = -\frac{\partial}{\partial x_i}(r^2\ln r) = -r_i(2\ln r + 1) \quad (14)$$

and in three dimensions ω_i is expressed as:

$$\omega_i = \frac{\partial}{\partial x_i}(r) = r_{,i} = \frac{r_i}{r} \quad (15)$$

Stress integral equation in terms of the heat source function is expressed as follows (Mohammadi et al., 2010):

$$\begin{aligned} \sigma_{ij}(\boldsymbol{\xi}) = \int_\Gamma \left(U_{ijk}^{*}t_k - S_{ijk}^{*}u_k\right)d\Gamma + \int_\Gamma \left(\lambda_{ij}^{*}\tfrac{\partial T}{\partial n} - \lambda_{ij}^{**}T\right)d\Gamma \\ + \tfrac{1}{k}\int_\Omega \lambda_{ij}^{*}g(\mathbf{x})d\Omega - \tfrac{E\alpha}{(1-2\nu)}T(\boldsymbol{\xi})\delta_{ij} \end{aligned} \quad (16)$$

where U^*_{ijk} and S^*_{ijk} are the commonly used functions in the BEM formulation of elastostatic problems (Aliabadi, 2002; Paris & Canas, 1997). The singular functions λ^*_{ij} and λ^{**}_{ij} are expressed for plane strain problems as (Mohammadi et al., 2010):

$$\lambda^*_{ij} = \frac{E\alpha}{4\pi(1-\nu)}\left[\left(\ln\frac{1}{r} - \frac{1+2\nu}{2}\right)\frac{\delta_{ij}}{(1-2\nu)} - r_{,i}r_{,j}\right] \tag{17}$$

$$\lambda^{**}_{ij} = \frac{E\alpha}{4\pi(1-\nu)r}\left[\left(2r_{,i}r_{,j} - \frac{\delta_{ij}}{1-2\nu}\right)\frac{\partial r}{\partial n} - (r_{,i}n_j + r_{,j}n_i)\right] \tag{18}$$

and for 3D problems as:

$$\lambda^*_{ij} = \frac{E\alpha}{8\pi(1-\nu)r}\left(\frac{\delta_{ij}}{1-2\nu} - r_{,i}r_{,j}\right) \tag{19}$$

$$\lambda^{**}_{ij} = \frac{E\alpha}{8\pi(1-\nu)r^2}\left[\left(3r_{,i}r_{,j} - \frac{\delta_{ij}}{1-2\nu}\right)\frac{\partial r}{\partial n} - (r_{,i}n_j + r_{,j}n_i)\right] \tag{20}$$

In the following sections, formulations for curved line heat sources in 2D and 3D thermoelastic problems are presented.

3. The formulation for curved line heat sources in 2D thermoelastic problems

Consider a curved line heat source in a 2D domain Ω as shown in Figure 1. The shape of the source and its intensity function can be arbitrary and sufficiently complicated. At first, a formulation for a quadratic line heat source is presented.

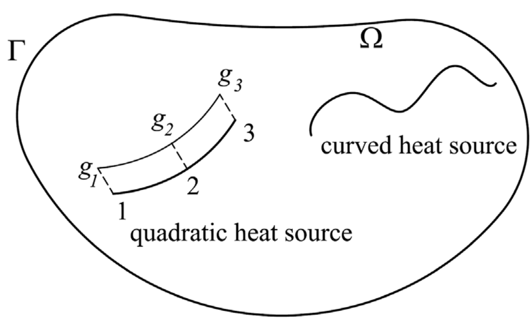

Figure 1. A 2D domain containing a curved line heat source with only one quadratic segment and a general curved line heat source.

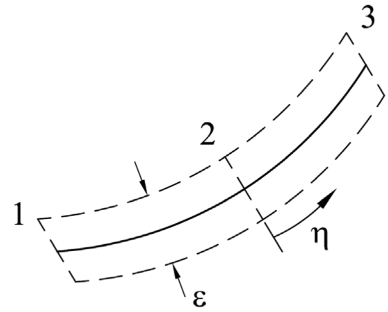

Figure 2. A quadratic heat source and its local coordinate system.

An arbitrary curved line heat source can be modelled by considering several quadratic heat sources. It is also assumed that the intensity of the source has a quadratic variation along the heat source.

The intensity per unit length of the quadratic source at the starting point (x_1, y_1), middle point (x_2, y_2) and end point (x_3, y_3) are represented by g_1, g_2 and g_3, respectively. This source is modelled as a distributed heat source over a quadratic curved region with infinitely small width ε as shown in Figure 2.

Considering Equation (6), the heat source integral in the temperature integral equation, i.e. Equation (5), becomes:

$$I_g = \frac{-1}{2\pi k} \int_{l_{source}} \frac{g(\mathbf{x})}{\varepsilon} \ln\left[r(\boldsymbol{\xi};\mathbf{x})\right] \varepsilon dl \tag{21}$$

Euclidian distance r from the singular point $\boldsymbol{\xi} = (x_s, y_s)$ to a point $\mathbf{x} = (x, y)$ on the quadratic heat source is:

$$r = \sqrt{(x - x_s)^2 + (y - y_s)^2} \tag{22}$$

x and y can be expressed as follows:

$$x = \sum_{n=1}^{3} N_n x_n \quad y = \sum_{n=1}^{3} N_n y_n \tag{23}$$

where the quadratic shape functions N_n are:

$$N_1 = \frac{1}{2}\eta(\eta - 1)\, N_2 = -(\eta + 1)(\eta - 1)\, N_3 = \frac{1}{2}\eta(\eta + 1) \tag{24}$$

η is a local coordinate attached to the quadratic heat source that varies from -1 to 1. The infinitesimal arc length dl can be written as:

$$dl = \sqrt{dx^2 + dy^2} = Jd\eta \tag{25}$$

where J is the Jacobian of transformation and can be expressed as:

$$J = \sqrt{\left(\sum_{n=1}^{3} x_n \frac{dN_n}{d\eta}\right)^2 + \left(\sum_{n=1}^{3} y_n \frac{dN_n}{d\eta}\right)^2} \tag{26}$$

Considering a quadratic variation for intensity of the heat source, $g(\mathbf{x})$ becomes:

$$g(\mathbf{x}) = \sum_{n=1}^{3} N_n g_n \tag{27}$$

Substituting Equation (25) and Equation (27) into Equation (21) leads to:

$$I_g = \frac{-1}{2\pi k} \int_{-1}^{1} \left(\sum_{n=1}^{3} N_n g_n\right) \ln\left[r(\eta)\right] J d\eta \tag{28}$$

By using Equation (14), Equation (25) and Equation (27), the heat source integral in the displacement integral equation, i.e. Equation (13) becomes:

$$I_{gi} = \frac{-\alpha(1+\nu)}{8\pi(1-\nu)k} \int_{-1}^{1} \left[\sum_{n=1}^{3} N_n g_n\right] \left[r_i(\eta)(2\ln\left[r(\eta)\right] + 1)\right] J d\eta \tag{29}$$

where r_i are

$$r_1 = (x - x_s),\ r_2 = (y - y_s) \tag{30}$$

Similarly, the heat source integral in the stress integral equation, i.e. Equation (16), can be expressed as:

$$I_{gij} = \frac{-E\alpha}{4\pi(1-\nu)k} \int_{-1}^{1} \left[\sum_{n=1}^{3} N_n g_n\right] \left[\left(\ln\left[r(\eta)\right] + \frac{1+2\nu}{2}\right)\frac{\delta_{ij}}{(1-2\nu)} + r_{,i}(\eta) r_{,j}(\eta)\right] J d\eta \tag{31}$$

Integrals in Equation (28), Equation (29) and Equation (31) can be evaluated using standard numerical integration methods.

4. The formulation for curved line heat sources in 3D thermoelastic problems

Consider a quadratic heat source in a 3D domain Ω. This source is modelled as a distributed heat source over a bar-like geometry with infinitely small radius ε as shown in Figure 3. The intensity per unit length of the quadratic heat source

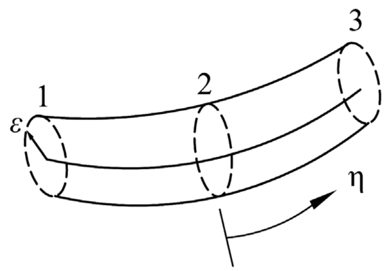

Figure 3. The local coordinate η along the 3D quadratic line heat source.

at the starting point (x_1, y_1, z_1), middle point (x_2, y_2, z_2) and end point (x_3, y_3, z_3) are g_1, g_2, and g_3, respectively.

Considering Equation (7), the heat source integral in the temperature integral equation, i.e. Equation (5), becomes:

$$I_g = \frac{1}{4\pi k} \int_{l_{source}} \frac{g(\mathbf{x})}{\pi\varepsilon^2} \frac{1}{r(\boldsymbol{\xi};\mathbf{x})} \pi\varepsilon^2 dl \tag{32}$$

Euclidian distance r from the singular point $\boldsymbol{\xi} = (x_s, y_s, z_s)$ to a point $\mathbf{x} = (x, y, z)$ on the quadratic heat source is:

$$r = \sqrt{\left(x - x_s\right)^2 + (y - y_s)^2 + (z - z_s)^2} \tag{33}$$

x, y and z can be written as:

$$x = \sum_{n=1}^{3} N_n x_n \quad y = \sum_{n=1}^{3} N_n y_n \quad z = \sum_{n=1}^{3} N_n z_n \tag{34}$$

where N_n are the quadratic shape functions, as expressed in Equation (24)

The infinitesimal arc length dl can be written as:

$$dl = \sqrt{dx^2 + dy^2 + dz^2} = Jd\eta \tag{35}$$

where J is the Jacobian of transformation and is expressed as follows:

$$J = \sqrt{\left(\sum_{n=1}^{3} x_n \frac{dN_n}{d\eta}\right)^2 + \left(\sum_{n=1}^{3} y_n \frac{dN_n}{d\eta}\right)^2 + \left(\sum_{n=1}^{3} z_n \frac{dN_n}{d\eta}\right)^2} \tag{36}$$

Substituting Equation (35) and Equation (27) into Equation (32) leads to:

$$I_g = \frac{1}{4\pi k} \int_{-1}^{1} \frac{\sum_{n=1}^{3} N_n g_n}{r(\eta)} Jd\eta \tag{37}$$

By using Equation (35), Equation (27) and Equation (15), the heat source integral in the displacement integral equation, i.e. Equation (13), becomes:

$$I_{gi} = \frac{\alpha(1+\nu)}{8\pi(1-\nu)k} \int_{-1}^{1} \frac{\sum_{n=1}^{3} N_n g_n}{r(\eta)} r_{i}(\eta) J d\eta \tag{38}$$

where r_i are

$$r_1 = (x - x_s),\ r_2 = (y - y_s),\ r_3 = (z - z_s) \tag{39}$$

Similarly, the heat source integral in the stress integral Equation (16) can be expressed as:

$$I_{gij} = \frac{E\alpha}{8\pi(1-\nu)k} \int_{-1}^{1} \frac{\sum_{n=1}^{3} N_n g_n}{r(\eta)} \left(\frac{\delta_{ij}}{1-2\nu} - r_{,i}(\eta) r_{,j}(\eta) \right) J d\eta \tag{40}$$

Similar to the 2D case, the integrals in Equation (37), Equation (38) and Equation (40) can be evaluated using standard numerical integration methods. The eight-point Gaussian integration method is used in this work.

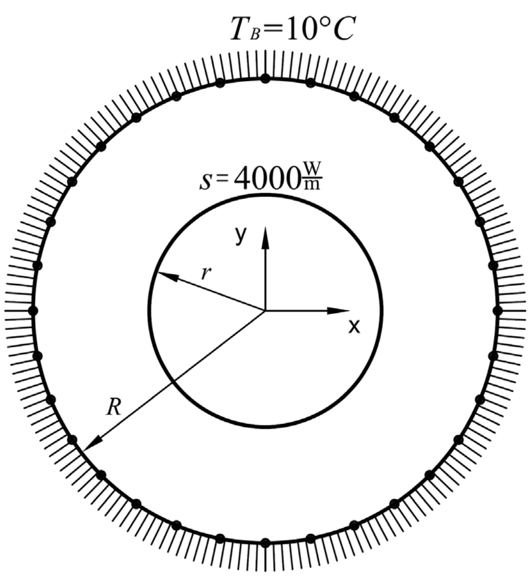

Figure 4. The BEM discretisation and boundary conditions of the circular domain with a circular heat source.

5. Numerical examples

In this part, two 2D examples and a 3D example are presented. In each example, the results obtained by the proposed BEM are compared with those of the FEM.

5.1. A circular heat source with uniform intensity in a circular domain

In the first example, a circular domain with $R = .5$ m is considered. The structural and thermal boundary conditions of the problem are shown in Figure 4. This problem is analysed under plane strain condition with $E = 200$ GPa, $\nu = .3$, $\alpha = 11.7 \times 10^{-6}\ \ 1/°\text{C}, k = 60\ \text{W}/\text{m}\ °\text{C}$ The problem boundary is modelled by 32 linear boundary elements. A curved heat source, which is distributed over a circle with radius $r = .25$ m is considered. The strength of the heat source is considered to be constant over the circle and equal to $s = 4000\ \text{Wm}^{-1}$.

In the BEM analysis, the circular heat source is modelled by only four quadratic heat sources. The acquired BEM results are compared with the FEM results obtained using ANSYS. In the FEM analysis, the circular heat source is modelled by a distributed heat source in a ring with a small width, $w = .01$ m. The FEM mesh (9461 quadratic elements) is shown in Figure 5.

The obtained results for the temperature, vertical displacement and the normal stress in the x- and y- directions, along the y-axis are shown in Figure 6. The results obtained by the proposed BEM show a good agreement with those of the FEM with the fine mesh.

Figure 6 implies that the presented BEM formulation yields accurate results for the distribution of the temperature, displacement and stress fields.

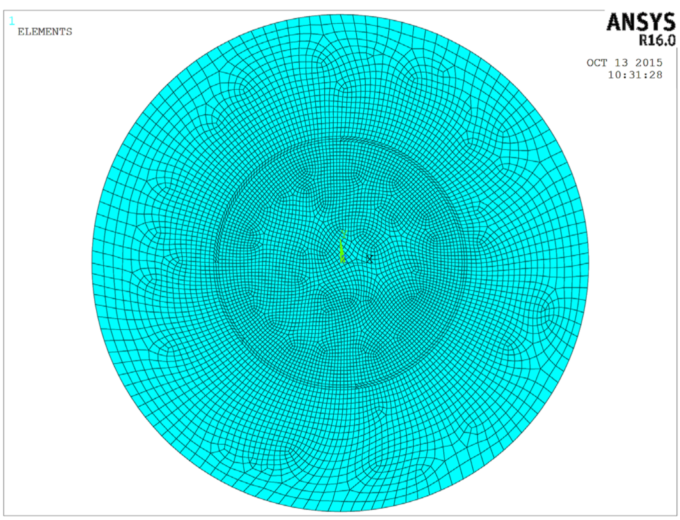

Figure 5. The FEM mesh of the circular domain with the circular heat source.

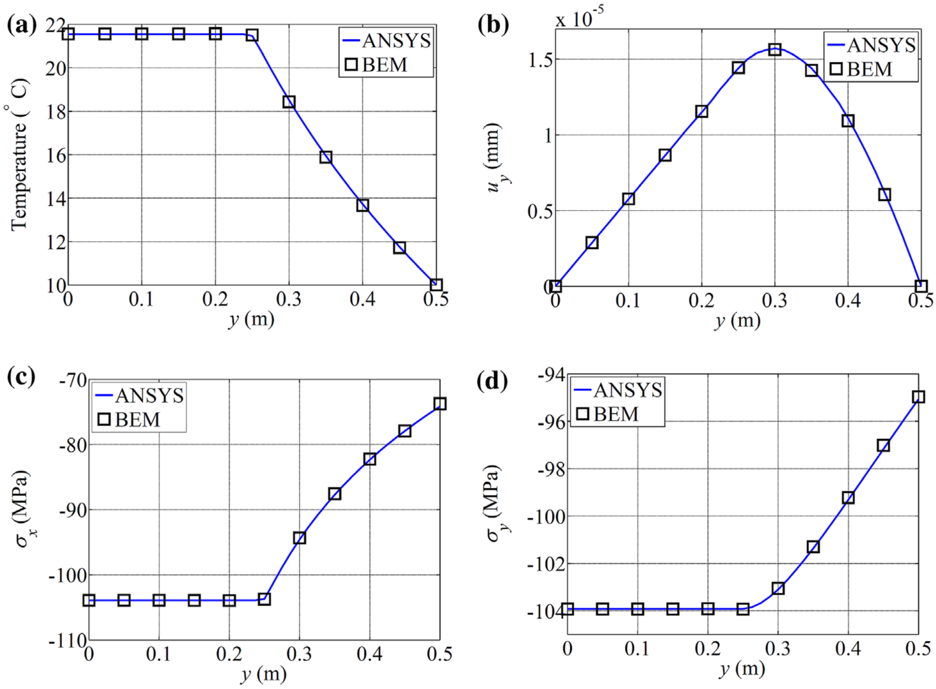

Figure 6. The FEM and BEM results along the y-axis for the first example: (a) temperature, (b) vertical displacement, (c) normal stress in the x-direction and (d) normal stress in the y-direction.

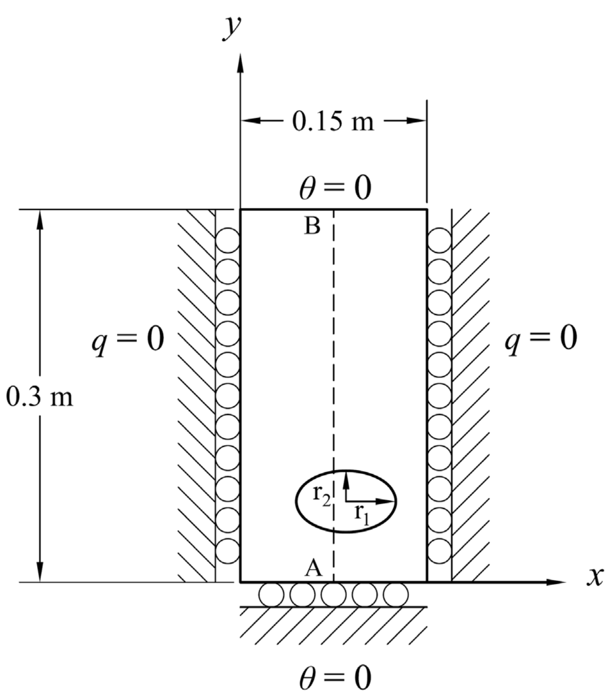

Figure 7. The problem geometry and boundary conditions of the rectangular domain with an elliptic heat source.

5.2. A heat source with an elliptical shape and non-uniform intensity in a rectangular domain

In the second example, a rectangular .15 m × .3 m domain is considered. The structural and thermal boundary conditions of the problem are shown in Figure 7. This problem is analysed under plane strain condition with $E = 200$ GPa, $\nu = .3$, $\alpha = 11.7 \times 10^{-6}\ \ 1/{}^\circ\text{C}$, $k = 60\ \text{W}/\text{m}\,{}^\circ\text{C}$. The problem boundary is modelled by 48 linear boundary elements. A curved heat source with an elliptical shape, centred at (.085, .065) is considered. The lengths of the major and minor radii of the ellipse are $r_1 = .04$ m and $r_2 = .02$ m, respectively.

The strength of the heat source is considered to be a function of $\beta \in [0 \quad 2\pi]$ with the following form:

$$s = 40,000[1 + \cos(\beta)] \quad (Wm^{-1}) \tag{41}$$

where β is the angular coordinate on the heat source, measured from the x-axis. In the BEM analysis, the elliptical heat source is modelled by only eight quadratic heat sources. The presented BEM results are compared with those of the FEM, obtained using ANSYS. In the FEM analysis, the elliptic heat source is modelled by a distributed heat source in an elliptic ring with a small width, $w = .0025$ m. The FEM mesh (4356 quadratic elements) is shown in Figure 8.

The obtained results for the temperature, vertical displacement, and the normal stress along line A-B are shown in Figure 9. Here again, the results obtained by the proposed BEM show a good agreement with those of the FEM with a fine mesh.

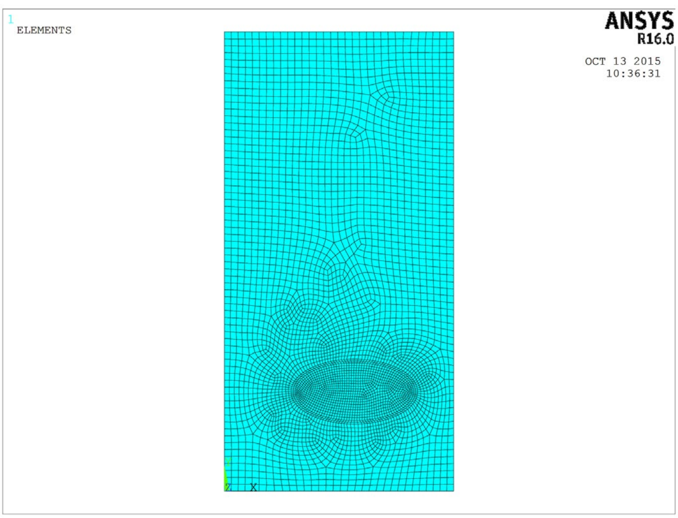

Figure 8. The finite element mesh of the rectangular domain with the elliptic heat source.

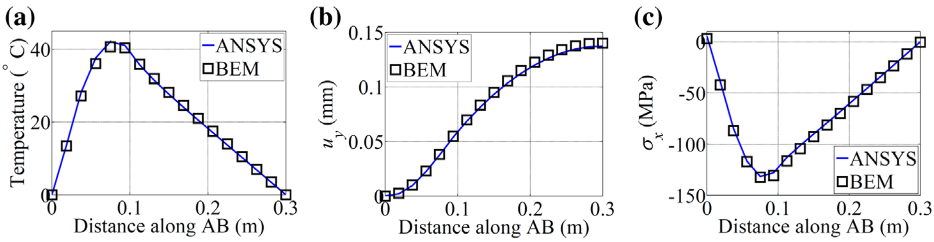

Figure 9. The FEM and BEM results along line A-B for the second example: (a) temperature, (b) vertical displacement and (c) normal stress in the *x*-direction.

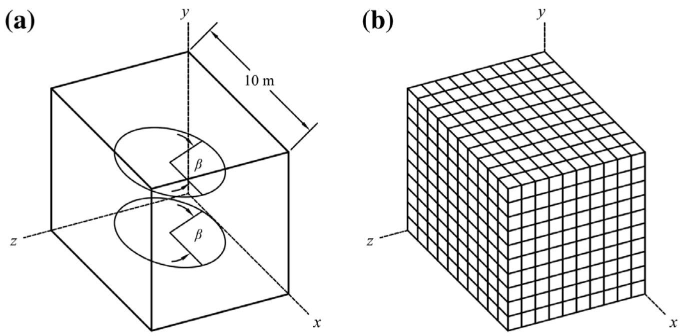

Figure 10. Schematic representation of (a) the problem domain and its geometry, and (b) the corresponding BEM discretisation.

5.3. Two circular heat sources with non-uniform intensity in a cube

In this example, a cube, of length $L = 10$ m, as shown in Figure 10, is considered. All faces are kept at $T = 0^{\circ}C$ and the displacements in the direction normal to all faces are zero. Thermomechanical properties of the material are $E = 200$ GPa, $\nu = .3, \alpha = 11.7 \times 10^{-6}\ {}^{1}/_{^\circ C}, k = 60\ \mathrm{W/m\,^\circ C}$. 600 constant boundary elements are used to model the problems with the BEM. This example problem is also analysed by the finite element method as a means of comparison of the numerical results. The commercial software package, ANSYS, is employed for the FE analysis; and quadratic 3D elements are utilised for meshing of the problem domain.

In this example, two curved heat sources, which are distributed over two circles with radius $R = 2.5$ m are considered. The first circular heat source is centred at (5,6,5) and the second one is centred at (5,4,5).

The strengths of the sources are considered to be functions of $\beta \in [0 \quad 2\pi]$ with the following forms:

$$\begin{aligned} s_1 &= 10000[1 + \cos(\beta)] \quad (\mathrm{Wm}^{-1}) \\ s_2 &= 20000[1 + \cos(\beta)] \quad (\mathrm{Wm}^{-1}) \end{aligned} \tag{42}$$

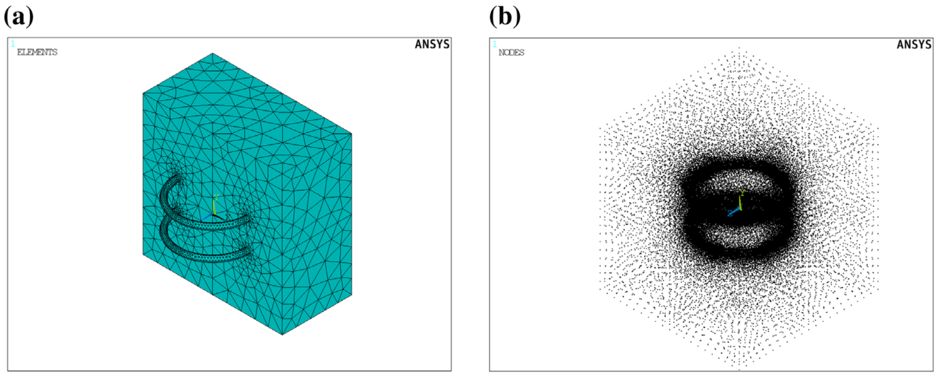

Figure 11. The FE mesh of the cube with two circular heat sources: (a) 56,669 quadratic 3D elements, and (b) 77,182 nodes.

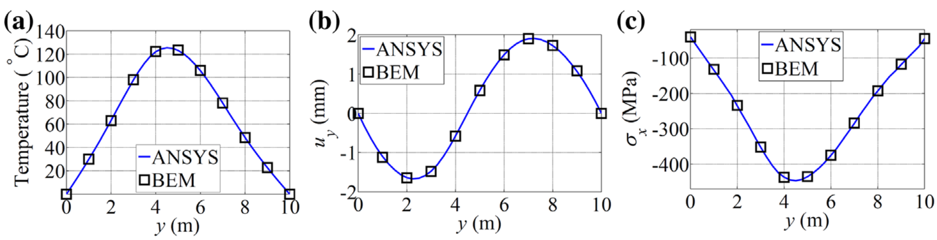

Figure 12. The BEM and FEM results for (a) the temperature, (b) the displacement in the *y*-direction and (c) the normal stress in the *x*-direction, along the line $x = z = 5$.

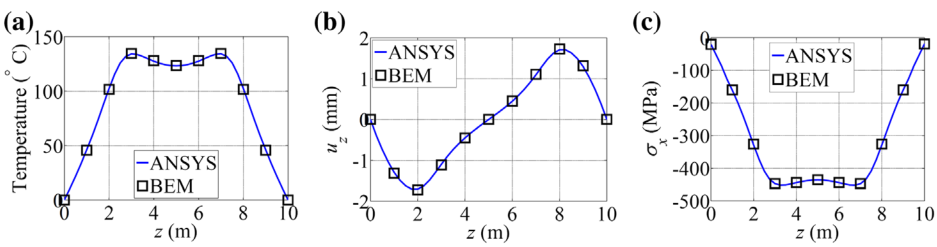

Figure 13. The BEM and FEM results for (a) the temperature, (b) the displacement in the *z*-direction and (c) the normal stress in the *x*-direction along the line $x = y = 5$.

where β is the angular coordinate on the heat sources, measured from the *x* axis (see Figure 10).

In the BEM analysis, each circular heat source is modelled by only four quadratic heat sources. The obtained BEM results are compared with those of the FEM. In the FEM analysis, each circular heat source is modelled by a distributed heat source in a torus with the small minor radius $r = .2$ m. The finite element meshing of the domain with quadratic 3D elements is shown in Figure 11. The whole domain is meshed with 56,669 quadratic elements and 77,182 nodes. In order to visualise the position of the curved heat sources inside the domain, only a cut-out of the FE mesh is shown in Figure 11(a). The nodal arrangement of the mesh is depicted in Figure 11(b).

The obtained results for the temperature, displacement and stress along the line $x = z = 5$ and the line $x = y = 5$ are shown in Figures 12 and 13, respectively. As it can be seen, the results obtained by the BEM are in an excellent agreement with the FEM solutions.

6. Conclusions

A boundary element formulation for the analysis of 2D and 3D thermoelastic problems in isotropic media containing internal curved line heat sources was presented. The shape of the curved line heat source can be arbitrary and complicated. The variation of the intensity of the curved line heat source can be arbitrary along the source as well. For accurate modelling of a curved line heat source in the domain methods such as the FEM, a distributed heat source over a small part of the domain and a large number of nodes should be considered. However, curved line heat sources can be efficiently modelled in the proposed BEM without considering additional degrees of freedom. Three examples were presented to show the effectiveness of the presented BEM formulation. The obtained numerical results show that the proposed method gives accurate results even with a small number of boundary elements. Extension of the proposed method to anisotropic thermoelastic problems can be useful too; however it is somewhat cumbersome because of the complicacy of the fundamental solutions for anisotropic problems.

Disclosure statement

No potential conflict of interest was reported by the authors.

ORCID

M. R. Hematiyan http://orcid.org/0000-0001-8926-7163
A. Khosravifard http://orcid.org/0000-0001-9835-8729

References

Aliabadi, M. H. (2002). *The boundary element method, applications in solids and structures* (Vol. 2). Chichester: John Wiley & Sons.

Chekurin, V. F., & Sinkevych, O. O. (2015). Boundary-element method of thermoelastic identification of cavities in long cylindrical bodies. *Journal of Mathematical Sciences, 205*, 667–676.

Cheng, A. H. D., Chen, C. S., Golberg, M. A., & Rashed, Y. F. (2001). BEM for thermoelasticity and elasticity with body force – A revisit. *Engineering Analysis with Boundary Elements, 25*, 377–387.

Gao, X. W. (2002). The radial integration method for evaluation of domain integrals with boundary-only discretization. *Engineering Analysis with Boundary Elements, 26*, 905–916.
Gao, X. W. (2003). Boundary element analysis in thermoelasticity with and without internal cells. *International Journal for Numerical Methods in Engineering, 57*, 975–990.
Gao, X. W., & Peng, H. F. (2011). Numerical evaluation of arbitrary singular domain integrals based on radial integration method. *Engineering Analysis with Boundary Elements, 35*, 587–593.
Hematiyan, M. R. (2007). A general method for evaluation of 2D and 3D domain integrals without domain discretization and its application in BEM. *Computational Mechanics, 39*, 509–520.
Hematiyan, M. R. (2008). Exact transformation of a wide variety of domain integrals into boundary integrals in boundary element method. *Communications in Numerical Methods in Engineering, 24*, 1497–1521.
Hematiyan, M. R., Mohammadi, M., & Aliabadi, M. H. (2011). Boundary element analysis of two-and three-dimensional thermo-elastic problems with various concentrated heat sources. *The Journal of Strain Analysis for Engineering Design, 46*, 227–242.
Hematiyan, M. R., Mohammadi, M., Marin, L., & Khosravifard, A. (2011). Boundary element analysis of uncoupled transient thermo-elastic problems with time-and space-dependent heat sources. *Applied Mathematics and Computation, 218*, 1862–1882.
Khan, O. U., & Yilbas, B. S. (2004). Laser heating of sheet metal and thermal stress development. *Journal of Materials Processing Technology, 155–156*, 2045–2050.
Liu, Y. J., Li, Y. X., & Huang, S. (2014). A fast multipole boundary element method for solving two-dimensional thermoelasticity problems. *Computational Mechanics, 54*, 821–831.
Mohammadi, M., Hematiyan, M. R., & Aliabadi, M. H. (2010). Boundary element analysis of thermo-elastic problems with non-uniform heat sources. *The Journal of Strain Analysis for Engineering Design, 45*, 605–627.
Neves, A. C., & Brebbia, C. A. (1991). The multiple reciprocity boundary element method in elasticity: A new approach for transforming domain integrals to the boundary. *International Journal for Numerical Methods in Engineering, 31*, 709–727.
Noda, N., Hetnarski, R. B., & Tanigawa, Y. (2003). *Thermal stresses* (2nd ed.). New York, NY: Taylor and Francis.
Nowak, A. J., & Brebbia, C. A. (1989). The multiple-reciprocity method. A new approach for transforming BEM domain integrals to the boundary. *Engineering Analysis with Boundary Elements, 6*, 164–167.
Ochiai, Y. (2001a). Steady heat conduction analysis in orthotropic bodies by triple-reciprocity BEM. *Computer Modeling in Engineering and Sciences, 2*, 435–445.
Ochiai, Y. (2001b). Two dimensional unsteady heat conduction analysis with heat generation by triple-reciprocity BEM. *International Journal for Numerical Methods in Engineering, 51*, 143–157.
Ochiai, Y. (2005). Three-dimensional steady thermal stress analysis by triple-reciprocity boundary element method. *International Journal for Numerical Methods in Engineering, 63*, 1741–1756.
Ochiai, Y., Sladek, V., & Sladek, J. (2013). Three-dimensional unsteady thermal stress analysis by triple-reciprocity boundary element method. *Engineering Analysis with Boundary Elements, 37*, 116–127.
Paris, F., & Canas, J. (1997). *Boundary element method*. Oxford: Oxford University Press.
Partridge, P. W., & Brebbia, C. A. (1990). Computer implementation of the BEM dual reciprocity method for the solution of general field equations. *Communications in Applied Numerical Methods, 6*, 83–92.

Partridge, P. W., Brebbia, C. A., & Wrobel, L. C. (1992). *The dual reciprocity boundary element method*. Southampton: Computational Mechanics Publications.
Rizzo, F. J., & Shippy, D. J. (1977). An advanced boundary integral equation method for three-dimensional thermoelasticity. *International Journal for Numerical Methods in Engineering, 11*, 1753–1768.
Shiah, Y. C., & Huang, J. H. (2005). Boundary element method interior stress/strain analysis for two-dimensional static thermoelasticity involving nonuniform volume heat sources. *Journal of Thermal Stresses, 28*, 363–390.
Shiah, Y. C., & Lin, Y. J. (2003). Multiple reciprocity boundary element analysis of two dimensional anisotropic thermoelasticity involving an internal arbitrary non-uniform volume heat source. *International Journal of Solids and Structures, 40*, 6593–6612.
Shiah, Y. C., & Tan, C. L. (2003). Determination of interior point stresses in two dimensional BEM thermoelastic analysis of anisotropic bodies. *International Journal of Solid and Structures, 37*, 809–829.
Shiah, Y. C., & Tan, C. L. (2012). Boundary element method for thermoelastic analysis of three-dimensional transversely isotropic solids. *International Journal of Solids and Structures, 49*, 2924–2933.
Shiah, Y. C., Guao, T. L., & Tan, C. L. (2005). Two-dimensional BEM thermoelastic analysis of anisotropic media with concentrated heat sources. *Computer Modeling in Engineering and Science CMES, 7*, 321–338.
Wrobel, L. C. (2002). *The boundary element method, applications in thermo-fluids and acoustics* (Vol. 1). Chichester: John Wiley & Sons.